Jain, M. and Roberts, J. and Ironside, C.N. (2005) Analysis of the gain distribution across the active region of InGaAs-InAlGaAs multiple quantum well lasers. *IEE Proceedings in Optoelectronics* 152:pp. 209-214.

http://eprints.gla.ac.uk/3944/

27th February 2008

Glasgow ePrints Service
https://eprints.gla.ac.uk

Analysis of the gain distribution across the active region of InGaAs-InAlGaAs multiple quantum well lasers

M. Jain, J. Roberts and C.N. Ironside

Abstract: Spectral gain measurements for two InGaAs-InAlGaAs multiple width quantum well structures, with inverse-configured active regions, have been presented. One structure consisted of wide quantum wells near the p-side and narrow quantum wells near the n-side of the active region. The other structure consisted of narrow quantum wells near the p-side of the active region with wider quantum wells near the n-side. It is shown that, for the same operating conditions, the structure with wide quantum wells on the p-side of the active region provided a 15% broader gain spectrum in comparison to the structure with narrow quantum wells on the p-side of the active region. The analysis of the results shows non-uniform carrier distribution across the active region of the structures, where the structure with wide quantum wells near the p-side of the active region provided 65% more gain in comparison to the structure with narrow quantum wells near the p-side of the active region. The gain distribution results have been compared with that obtained for the phosphorous quaternary structures in other literature and have shown there is some evidence to suggest that the gain distribution is more uniform in aluminium quaternary than phosphorous quaternary material.

1 Introduction

In order to design a multiple quantum well (MQW) laser to operate effectively, where all quantum wells in the active region contribute equally to the material gain, a good understanding of the spatial distribution of carriers through the active region is required. There is experimental and theoretical evidence that there is a non-uniform distribution of carriers, where the gain contribution from different wells varies within the same active region, resulting in a reduction of the number of effectively working quantum wells [1]. In this paper we present evidence that, for optical communication MQW lasers operating around 1550 nm, it is possible to have a more uniform distribution of carriers with the InAlGaAs (aluminium-quaternary) than has been previously reported for the InGaAsP (phosphorous-quaternary) material devices.

In the past, for semiconductor lasers operating at telecommunication wavelengths (1300–1550 nm), much of the research and development effort have been devoted to phosphorous-quaternary-based QW lasers. However, the direct bandgap aluminium-quaternary material system, lattice matched to InP-based substrates, has in recent years started to yield productive results and is gaining attention for use in optical communications systems. Our main goal in this paper was to investigate the optical gain distribution across the active region of an aluminium-quaternary MQW structure with respect to the current injection, which may provide an insight into the distribution of carriers across the active region in this structure. The importance of this work is highlighted by the problem of non-uniform carrier distribution in conventional phosphorous-quaternary material, where previous work on deep valence band-offset in InGaAsP material reported it being a detrimental factor to device performance [2]. For the same total bandgap difference between the well and the barrier layers, an InAlGaAs material system provides larger conduction band discontinuity of $E_c/E_g = 0.72$, in comparison to the value of $E_c/E_g = 0.40$ for an InGaAsP material system, hence providing better electron confinement in the conduction band [3].

To study gain distribution in an aluminium-quaternary material system, two InGaAs-InAlGaAs multiple width quantum wells (MWQW) structures (also referred to as asymmetric quantum well structure [4]) were grown by metal-organic vapour phase epitaxy (MOVPE), with operating wavelength centred around 1550 nm. These two structures were identical except for having inverse-configured quantum wells in their active region; in other words (for example), if one structure has three QWs configured in the sequence of decreasing size from the p-side to the n-side of the active region, the second structure has the QWs configured in the sequence of increasing size. The technique of employing inverse-configured quantum wells in an active region has been used previously in various material systems to study the carrier distribution across the active region of an MQW laser [2, 5, 6]. These MWQW lasers are also of interest because they have been used as broad bandwidth lasers to obtain increased tuning range [7] and for mode-locking to obtain decreased pulse width [8]. With our goal in mind, we employed the two MWQW structures to carry out

© IEE, 2005

IEE Proceedings online no. 20045069

doi: 10.1049/ip-opt:20045069

Paper first received 12th December 2004 and in revised form 19th April 2005. Originally published online 16th June 2005

M. Jain is with the Institute of Applied Physics, University of Regensburg, 93040 Germany

J. Roberts is with the Department of Electronics Engineering, University of Sheffield, Sheffield S1 3JD, UK

C.N. Ironside is with the Department of Electronics and Electrical Engineering, University of Glasgow, Glasgow G12 8LT, Scotland, UK

E-mail: manish.jain@myrealbox.com

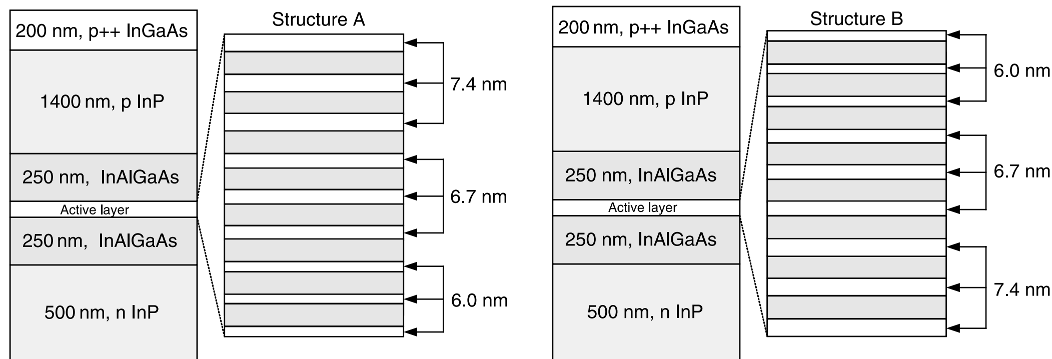

Fig. 1 *InGaAs-InAlGaAs MWQW structures*

Structure A has wide quantum wells near the p-side and narrow quantum wells near the n-side of the active region. Structure B has an inverse configuration of quantum wells compared to A

spectral gain measurements and analyse the spectral gain data obtained from this experiment.

2 Wafer structures

The two inverse-configured structures we employed for the spectral gain measurements are referred to as structures A and B, as shown in Fig. 1. The growth of both the MWQW wafer structures was undertaken on n-doped InP substrates by MOVPE, at 150Torr using low-oxygen-containing alkyls, at the III-V semiconductor facility at Sheffield University. Both wafers consisted of heavily p-doped ($5 \times 10^{18}\,cm^{-3}$) InGaAs contact layers; p and n-doped InP cladding layers ($2 \times 10^{18}\,cm^{-3}$) and un-doped InAlGaAs waveguide core, with the active region placed at the centre of the core. The active region of the two inverse-configured MWQW wafers consisted of three 6 nm, three 6.7 nm and three 7.4 nm latticed matched $In_{0.53}Ga_{0.47}As$ quantum wells. As seen from Fig. 1, structure A had the widest QWs (7.4 nm in width) in the p-side of the active region, whereas structure B had the narrowest QWs (6.0 nm in width) in the p-side of the active region. In both the structures, the QWs were separated by 9 nm-wide InAlGaAs barriers. The optical confinement factor calculated for each of our MWQW devices is 0.1206.

To calculate the energy gap between E_1-HH_1 transition for quantum wells of width 6, 6.7 and 7.4 nm, a Schrödinger Numerical Problem Solver was used. Using the material parameters for $In_{0.53}Ga_{0.47}As/In_{0.53}Al_{0.20}Ga_{0.27}As$ shown in Table 1, the energy gap calculated for 6, 6.7 and 7.4 nm-wide quantum wells is 807, 794, and 785 meV respectively. With respect to the experiment, these calculated values are intended to be indicative since the many-body processes [9] can change the operating wavelengths for the respective quantum wells in the MWQW structures. The material parameters for phosphorus-quaternary, calculated for a similar energy band gap to aluminium-quaternary material, are also given in Table 1 for reference.

Table 1: Material parameters

Physical property	Value
$In_{0.53}Ga_{0.47}As$ parameters[a] (quantum well region)	
Energy band gap (eV) at 300 K	0.75
Electron effective mass ($1/m_0$)	0.041
Heavy hole effective mass ($1/m_0$)	0.46
Light hole effective mass ($1/m_0$)	0.0503
$In_{0.53}Al_{0.20}Ga_{0.27}As$ parameters[b] (barrier region)	
Energy band gap (eV) at 300 K	1.0056
Electron effective mass ($1/m_0$)	0.0605
Heavy hole effective mass ($1/m_0$)	0.5055
Light hole effective mass ($1/m_0$)	0.0675
$In_{0.72}Ga_{0.28}As_{0.60}P_{0.40}$ parameters[b] (barrier region)	
Energy band gap (eV) at 300 K	1.0056
Electron effective mass ($1/m_0$)	0.0595
Heavy hole effective mass ($1/m_0$)	0.5292
Light hole effective mass ($1/m_0$)	0.0775

[a] $In_{0.53}Ga_{0.47}As$ parameters obtained from [10].
[b] $In_{0.53}Al_{0.20}Ga_{0.27}As$ and $In_{0.72}Ga_{0.28}As_{0.60}P_{0.40}$ material parameters are calculated using interpolation formulas mentioned in [3].

3 Photoluminescence analysis

The photoluminescence (PL) measurements (Fig. 2) were carried out to assess the emission wavelength of structures A and B where the carriers are distributed more equally across the active region than under electrical injection. These measurements were performed at the same operating conditions, at 77 K and 300 K, using an Argon (514 nm) laser which excited carriers in both wells and barriers. It can be seen that the full-width half-maximum (FWHM) obtained for structure A (Figs. 2*a* and *b*) are approximately 5–10% broader than that obtained for structure B (Figs. 2*c* and *d*). From Figs. 2*a* and *b*, the FWHM at 77 K and 300 K for structure A is 45 nm and 100 nm respectively. The emission peaks at 77 K and 300 K are 1420 and 1515 nm respectively. From Figs. 2*c* and *d*, the FWHM measured for structure B is 40 nm and 96 nm at 77 K and 300 K respectively. The peak emissions at 77 K and 300 K, for structure B, are at 1424 nm and 1510 nm, respectively. Since both A and B have an equal number of QWs and are nominally identical in dimensions and compositions, the PL spectra obtained for them differ in the range of 5–10%, hence implying a nearly similar growth quality for both structures. The difference of 5–10% (approximately 4–5 nm for both 300 K and 77 K) is likely to be within the margin of error; however these differences may have also occurred as a result of slight differences in growth conditions of both the structures.

4 Spectral gain measurements and discussion

The spectral gain measurements in our experiment were carried out using a multi-section device technique mentioned in [11]. The gain measurements were carried out under

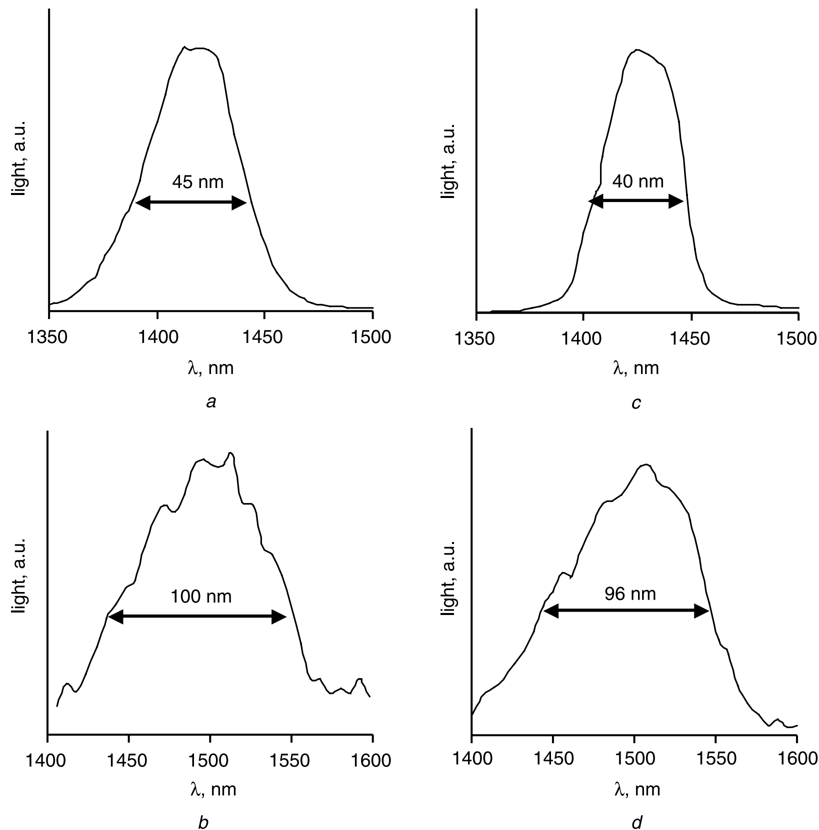

Fig. 2 *Photoluminescence spectra*

a Structure A at 77 K
b Structure A at 300 K
c Structure B at 77 K
d Structure B at 300 K

pulsed current injection with the devices being temperature controlled and all the data taken at room temperature. The devices fabricated from structures A and B, for this experiment, are referred to as devices A and B, respectively. The TE gain spectra, obtained below the threshold for both the devices are shown in Fig. 3. The three vertical lines included in the gain spectra corresponds to the calculated energy gap between E_1-HH_1 transition for the 6.0, 6.7 and 7.4 nm QWs included in the active region of both structures A and B, as mentioned previously in Section 2.

The transparency current density, J_t, where the semiconductor material gain is transparent, for structures A and B were estimated to be $2.3\,kAcm^{-2}$ and $1.3\,kAcm^{-2}$, respectively [12], where they were calculated using the TE net modal gain and internal optical losses data of both structures. The mismatch in the transparency current density by a factor of two probably resulted because of higher diode turn-on voltage obtained for device A (1.5 Volts) in comparison to that for device B (0.7 Volts), measured in our preliminary experiments. The active region of device A appears to be unaffected by high diode turn-on voltage as the gain spectra for device A (Fig. 3*a*) shows inhomogeneous broadening with increasing current injection (resulting from the inclusion of the three multiple width quantum wells) and is centred around the expected 1550 nm wavelength. A possible explanation for the high diode turn-on voltage obtained for device A is because of lower than designed doping concentration in either (or both) the contact $(5 \times 10^{18}\,cm^{-3})$ and upper-cladding $(2 \times 10^{18}\,cm^{-3})$ layers. This results in a significant proportion of voltage drop across the contact and upper cladding layers of device A without having any major affect on the active region.

Following are the relevant observations made from the TE gain spectra:

(1) The inhomogeneous spectral gain broadening is evident from relatively broad gain spectra, for both the devices, resulting from the inclusion of three sets of multiple width wells.
(2) The widest 7.4 nm quantum wells, with lower density of states than 6.7 and 6.0 nm wells, contributes to net modal gain at lower current density compared to the narrow QWs. This is followed by net modal gain contribution from 6.7 and 6.0 nm QWs at current injection of: i) 1.6 and just below $2.4J_t$, respectively, for device A; ii) 1.1 and $1.5J_t$, respectively for device B.
(3) For device A, the TE gain peak is centred around the 6.7 nm QWs, between current densities 2.4–$4.0J_t$. For device B, the TE peak gain is centred around 6.7 nm QWs between current injection of 1.9–$2.3J_t$, however the gain peak shifts to the narrowest 6.0 nm QWs when the QWs are pumped to higher current injection $(3.1$–$3.8J_t)$.
(4) The proportion of gain contribution, from 6.0, 6.7 and 7.4 nm QWs in device A is more even than device B. For example, the peak gain contribution obtained, at current density injection of $4J_t$, from 7.4, 6.7 and 6.0 nm QWs is 48.8, 63.7 and $57.9\,cm^{-1}$ respectively; whereas the gain contribution from 6.0, 6.7 and 7.4 nm QWs in the active region of device B, for approximately similar operating condition, is 65.4, 53.8 and $28.6\,cm^{-1}$, respectively.

If the carrier distribution across the active region of an MQW structure were uniform then the two structures, which are identical except for the configuration of quantum wells (one of the structures has an inverse arrangement of the QWs

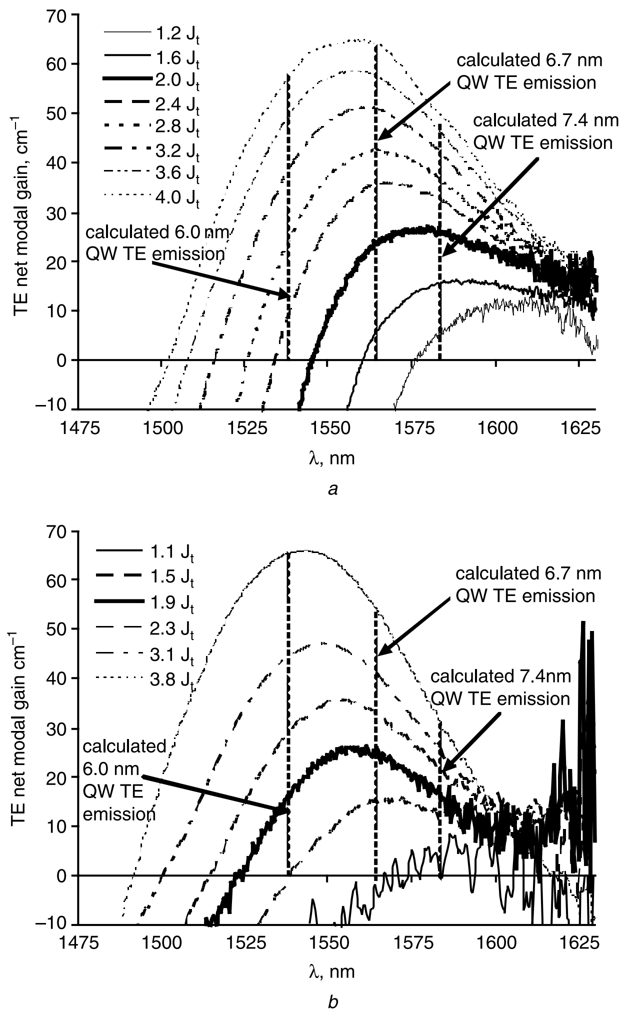

Fig. 3 *TE net modal gain spectra*
a Device A (with $J_t = 2.3\,kAcm^{-2}$)
b Device B (with $J_t = 1.3\,kAcm^{-2}$)
J_t is the transparency current density

of the second structure), would have similar gain spectra under the same operating conditions. However, observations made from Fig. 3 shows that the gain spectra obtained for both devices A and B are not similar, indicating a variation of the carrier distribution across the active region of both the structures with the change in the quantum well configuration in the active region.

Figure 4 shows a comparison between the peak gain contribution from 7.4, 6.7 and 6.0 nm QWs in both devices. This was examined to evaluate the importance the carrier distribution has on the gain contribution from each part of the active region when the quantum well configuration is reversed. The black line in the plot shows a good logarithmic fit corresponding to the experimental values obtained from both the devices, a feature generally observed in MQW lasers [13].

From Fig. 4*a*, the wide 7.4 nm QWs in device A, located near the p-side of the active region, contribute to, on average, 65% more gain between 2.3–4.0J_t, in comparison to the 7.4 nm QWs located near the n-side of the active region of device B. Observations made from Fig. 4*c* show that, at current injection of approximately 2.3J_t, the narrow 6.0 nm QWs, located near the p-side of the active region in device B, contribute to around three times more gain in comparison to the 6.0 nm QWs located near the n-side of the active region in device A. However, at high current injection (4J_t), this difference in the gain contribution decreases to 20%. Finally from Fig. 4*b*, the 6.7 nm QWs, which are located in the centre of the active region in both the devices, show the least difference (ranging between 6–10%) in the gain contribution, in comparison to the observations made from Fig. 4*a* for 7.4 nm QWs and Fig. 4*c* for 6.0 nm QWs. The fact there is little difference for the centre wells (6.7 nm) between the samples suggests that the experimental technique gives approximately consistent results.

Normalised gain concentration distribution across the active region of 7.4 nm and 6.0 nm structures is plotted with respect to current density and QWs location in the active region (Fig. 5) to obtain an insight into the gain distribution across a conventional InGaAs-InAlGaAs MQW structure. This was plotted with the experimental gain data obtained for both MWQW devices and using the gain at the centre of the active region as the calibration point, where the gain is approximately same between the samples. From Fig. 5, it is observed that the uniformity of the gain concentration across the active region of a conventional MQW structure is dependent on the width of the QW. For the wide 7.4 nm MQW structure, the proportion of the gain distribution across the active region is approximately the same for varying current injection, with the gain concentration being 65% larger on the p-side than the n-side of the active region. For the narrow 6.0 nm MQW structure, however, the gain distribution is strongly uneven at lower current injection (2.4J_t) but appears to become more uniform at higher current injection (3–3.8J_t). The difference between the two bar charts for wide 7.4 nm QW and narrow 6.0 nm QW indicates that, at high current injection, the gain concentration can be as high as 40% more uniform across the active region of a narrow 6.0 nm than wide 7.4 nm InGaAs-InAlGaAs MQW structure.

In order to compare the spectral gain bandwidth obtained for both the MWQW devices A and B, we calculated the full width half maximum (FWHM) of the TE gain spectra (Fig. 3), at different current injections, as shown in Fig. 6*a*. From Fig. 6*a*, at lower current injection ($<2.5J_t$), both devices have approximately matching FWHM. However, with increasing current density injection, the FWHM obtained for device A gets slightly wider in comparison to device B. For example, at a current density injection of 4J_t, the FWHM obtained for device A is 86 nm in comparison to 75 nm obtained for device B, thus 15% wider.

Figure 6*b* shows the spontaneous emission spectra for both devices. It can be clearly seen from Fig. 6*b* that the emission peaks for both devices correspond to the 6.7 nm and 6.0 nm QWS, in the respective active regions of both devices. In addition, device A provides approximately 19% broader spontaneous emission spectra than device B, a value closely matched to the 15% broader gain spectra obtained for device A in comparison to device B. The centre operating wavelength varies depending on the QW located near the p-side of the active region.

Observations made from all our results do indicate that the QWs near the p-side of the active region, in aluminium-quaternary material, do assist in providing a larger gain contribution than QWs near the n-side; this aspect is stronger for wide QWs near the p-side than the narrow QWs where a 15% wider gain spectra was obtained by including wide QWs near the p-side than the n-side. Similar behaviour in inverse-structures has been reported previously [5, 14] where a MWQW structure with a wide well on the p-side provides broader gain spectrum than having narrow wells on the p-side.

We compared the gain contribution difference of 65% obtained between the widest 7.4 nm QWs in both our aluminium-quaternary inverse MWQW structures with that reported by Hamp *et al.* [15, 16], under similar conditions

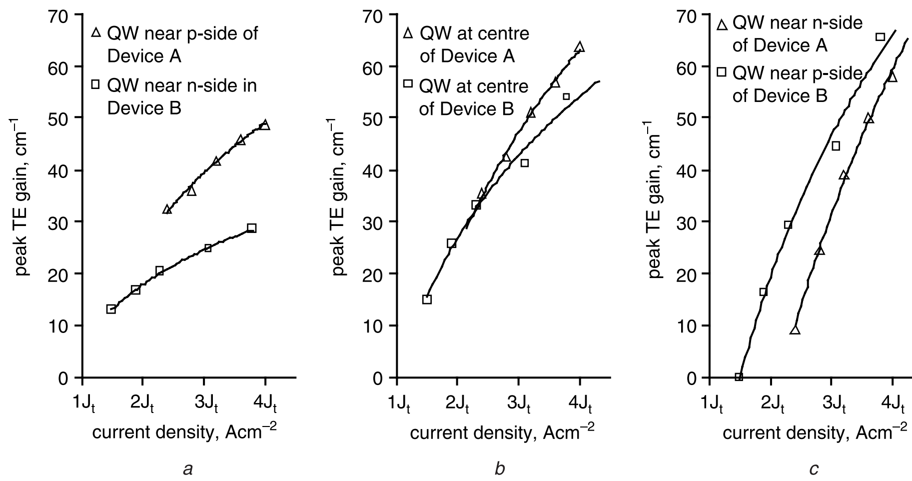

Fig. 4 *Peak TE gain comparison of QWs in the active region of devices A and B against current density*

a 7.4 mm QWs
b 6.7 nm QWs
c 6.0 nm QWs

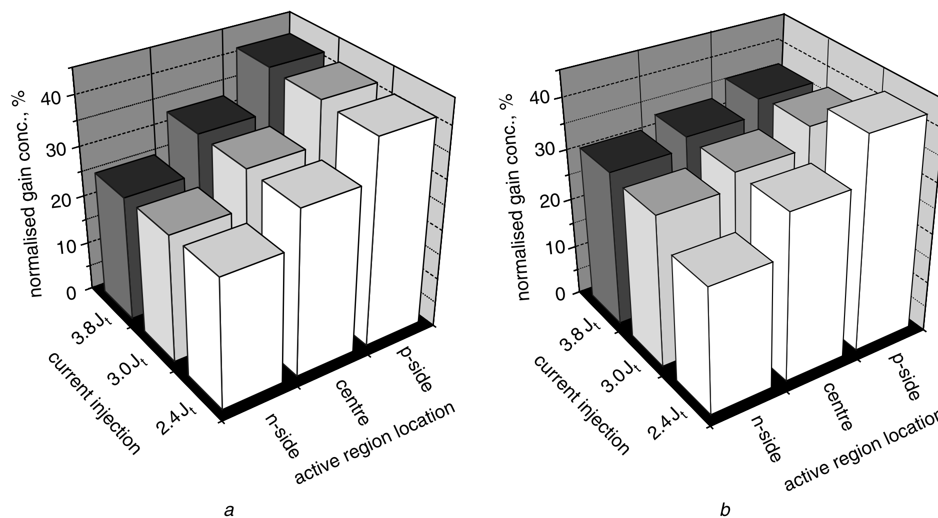

Fig. 5 *Normalised gain concentration for InGaAs-InAlGaAs multi-quantum well structure*

a 7.4 nm MQW structure
b 6.0 nm MQW structure

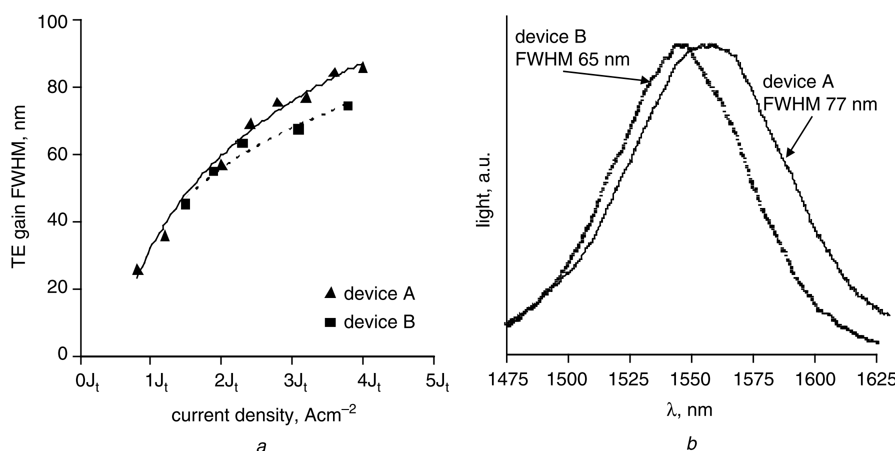

Fig. 6 *FWHM of gain spectra against J_t and spontaneous emission spectra*

a FWHM of gain spectra against J_t, where J_t is the transparency current density, for device A $J_t = 2.3\,kAcm^{-2}$ and device B $J_t = 1.3\,kAcm^{-2}$
b Spontaneous emission spectra of devices A and B at $0.5J_t$

using the inverse-configuration technique, who carried out research into the gain contribution across the active region of MWQW phosphorous-quaternary lasers at around 1550 nm. The comparison was carried out ensuring that the physical dimensions of the phosphorous-quaternary active region (width of QWs and barriers) closely matched those of the aluminium-quaternary structures employed in our experiment.

Hamp *et al.* [15] studied two inverse InGaAsP MWQW structures with the active region consisting of four wells in total with two sets of MWQW of widths 10 nm and 5 nm. These QWs were separated by 10 nm-wide barriers. They reported a 74% larger gain contribution from the wide 10 nm QWs when located near the p-side of the active region than the net gain contribution from those QWs when located near the n-side. This mismatch in the gain contribution between the wide QWs in the inverse-configured structures is about 9% larger than obtained in our case. They succeeded in reducing the gain contribution difference between the wide QWs in their MWQW inverse structures from 74% to 18% by reducing the barrier width from 10 nm to 5 nm. It has been previously reported that the non-uniformity of carriers increases with the number of QWs [16, 17]. Since we employed more than twice as many wells in our MWQW structure than the number of wells employed in the above mentioned InGaAsP structure [15], the gain contribution difference between the wide QWs in the inverse-configured InGaAsP structure could possibly be larger than 9% in comparison to our aluminium-quaternary structure. In the other case [16], they employed two inverse-configured InGaAsP MWQW structures with ten QWs in the active region with three different sets of MWQW, separated by 10 nm-wide barriers. In their experiment, they obtained 108 % higher gain from the widest QWs when located near the p-side of the active region than in the inverse configuration when the widest QWs were located near the n-side. These are larger differences than we report here with the aluminium-quaternary material and although these structures are not strictly comparable they provide some evidence that the gain is more uniform in the aluminium-quaternary material.

5 Conclusions

Spectral gain measurements have been carried out on two inverse-configured aluminium-quaternary MWQW structures. Observations made from the TE gain spectra showed that the structure with wider quantum wells near the p-side of the active region provided 15% wider gain spectrum in comparison to the structure with narrow quantum wells on the p-side. Ideally, with uniform carrier distribution, the inverse-configured structures in our experiment should have provided identical gain spectra. However it is important to realise that although the gain spectra obtained for devices A and B are not identical, a small difference of 15% in the FWHM of the gain spectrum, obtained for our inverse-configured devices, in fact highlights a possible underlying advantage of employing aluminium-quaternary material in the active region, where shallower valence band-offset facilitates in providing uniform carrier distribution in comparison to the conventional phosphorus-quaternary QW material. The result also emphasises the problem of non-uniform carrier distribution in an active region of a structure, where, for the given current densities, the gain contribution from the 7.4 and 6.0 nm wells near the p-side of the active region provided 65% and 20%, respectively, more gain than wells on the n-side of the active region.

In addition, a small mismatch of 6–10% in the gain contribution from the 6.7 nm QWs located in the centre of the active region of both the structures justified the process of employing an inverse-configured technique for studying the gain contribution from the QWs in the active region. It would be reasonable to assume that the gain contribution from the 6.7 nm QWs in both the inverse-configured MWQW structures should be closely matched at similar operating conditions. Experimental results from our spectral gain measurements on aluminium-quaternary devices indicates uniformity of gain contribution, from the QWs across the active region, ranging between 9–34% higher than the work reported on gain contribution from QWs in the phosphorus-quaternary devices.

6 Acknowledgments

We gratefully acknowledge the Engineering and Physical Science Research (EPSRC) council for financial support and for a studentship for M. Jain to carry out this work in the Department of Electronics and Electrical Engineering, University of Glasgow.

7 References

1 Ban, D., and Sargent, E-H.: 'Influence of nonuniform carrier distribution on the polarization dependence of modal gain in multi-quantum-well lasers and semiconductor optical amplifiers', *IEEE J. Quantum Electron.*, 2000, **36**, (9), pp. 1081–1088
2 Yamazaki, H., Tomita, A., Yamaguchi, M., and Sasaki, Y.: 'Evidence of nonuniform carrier distribution in multiple quantum well lasers', *Appl. Phys. Lett.*, 1997, **71**, (6), pp. 767–769
3 Li, E.H.: 'Material parameters of InGaAsP and InAlGaAs systems for use in quantum well structures at low and room temperatures', *Physica E*, 2000, **5**, pp. 215–273
4 Hamp, M.J., Cassidy, D.T., Robinson, B.J., Zhao, Q.C., Thompson, D.A., and Davies, M.: 'Effect of barrier height on the uneven carrier distribution in asymmetric multiple-quantum-well InGaAsP lasers', *IEEE Photon. Technol. Lett.*, 1998, **10**, (10), pp. 1380–1382
5 Park, Y.H., Kang, B-K., Lee, S., Woo, D.H., and Kim, S.H.: 'Structure of the quantum well for a broad-band semiconductor optical amplifier', *J. Korean Phys. Soc.*, 2000, **36**, (4), pp. 206–208
6 Newell, T.C., Wright, M.W., Hou, H., and Lester, L.F.: 'Carrier distribution, spontaneous emission and gain engineering in lasers with nonidentical quantum wells', *IEEE J. Sel. Top. Quantum Electron.*, 1999, **5**, (3), pp. 620–626
7 Woodworth, S.C., Cassidy, D.T., and Hamp, M.J.: 'Experimental analysis of a broadly tunable InGaAsP laser with compositionally varied quantum wells', *IEEE J. Quantum Electron.*, 2003, **39**, pp. 620–626
8 Jain, M., McDougall, S.D., Bryce, A.C., and Ironside, C.N.: 'Investigation of spectrally broad gain multiple-width quantum well material for colliding pulse mode-locked operation', *IEE Proc. Optoelectron.*, 2004, **151**, pp. 133–137
9 Haug, H., and Koch, S.W.: 'Semiconductor laser theory with many-body effects', *Phys. Rev. A, Gen. Phys.*, 1989, **39**, pp. 1887–1898
10 Chuang, S.L.: 'Physics of optoelectronic devices' (Wiley-Interscience Publication, 1995), p. 711
11 Thomson, J.D., Summers, H.D., Hulyer, P.J., Smowton, P.M., and Blood, P.: 'Determination of single-pass optical gain and internal loss using a multisection device', *Appl. Phys. Lett.*, 1999, **75**, pp. 2527–2529
12 Jain, M.: 'An investigation of broad gain spectrum InGaAs/InAlGaAs quantum well lasers latticed matched to InP', PhD thesis, University of Glasgow, 2002
13 Whiteaway, J., Thompson, G., Greene, P., and Glew, R.: 'Logarithmic gain/current-density characteristics of InGaAs/InGaAlAs/InP multi-quantum-well separate-confinement-heterostructure lasers', *Electron. Lett.*, 1991, **27**, (4), pp. 340–342
14 Hamp, M.J., and Cassidy, D.T.: 'Experimental and theoretical analysis of the carrier distribution in asymmetric multiple quantum-well InGaAsP lasers', *IEEE J. Quantum Electron.*, 2001, **37**, (1), pp. 92–99
15 Hamp, M.J., Cassidy, D.T., Robinson, B.J., Zhao, Q.C., and Thompson, D.A.: 'Effect of barrier thickness on the carrier distribution in asymmetric multiple-quantum-well InGaAsP lasers', *IEEE Photon. Technol. Lett.*, 2000, **12**, (2), pp. 134–136
16 Hamp, M.J., Cassidy, D.T., Robinson, B.J., Zhao, Q.C., and Thompson, D.A.: 'Nonuniform carrier distribution in asymmetric multiple-quantum-well InGaAsP laser structures with different number of quantum wells', *Appl. Phys. Lett.*, 1999, **74**, (5), pp. 744–746
17 Lin, C.H., Chua, C.L., Zhu, Z.H., and Lo, Y.H.: 'On nonuniform pumping for multiple-quantum well semiconductor lasers', *Appl. Phys. Lett.*, 1994, **65**, (19), pp. 2383–2385